

UNCLASSIFIED

Defense Technical Information Center
Compilation Part Notice

ADP012587

TITLE: The Role of Nitrogen-Induced Localization and Defects in InGaAsN [2% N]: Comparison of InGaAsN Grown by Molecular Beam Epitaxy and Metal-Organic Chemical Vapor Deposition

DISTRIBUTION: Approved for public release, distribution unlimited

This paper is part of the following report:

TITLE: Progress in Semiconductor Materials for Optoelectronic Applications Symposium held in Boston, Massachusetts on November 26-29, 2001.

To order the complete compilation report, use: ADA405047

The component part is provided here to allow users access to individually authored sections of proceedings, annals, symposia, etc. However, the component should be considered within the context of the overall compilation report and not as a stand-alone technical report.

The following component part numbers comprise the compilation report:

ADP012585 thru ADP012685

UNCLASSIFIED

The Role of Nitrogen-Induced Localization and Defects in InGaAsN ($\approx 2\%$ N): Comparison of InGaAsN Grown by Molecular Beam Epitaxy and Metal-Organic Chemical Vapor Deposition

Steven R. Kurtz, A. A. Allerman, J. F. Klem, R. M. Sieg, C. H. Seager, and E. D. Jones
Sandia National Laboratories, Albuquerque, NM 87185-0601

Abstract

Nitrogen vibrational mode spectra, Hall mobilities, and minority carrier diffusion lengths are examined for InGaAsN (≈ 1.1 eV bandgap) grown by molecular beam epitaxy (MBE) and metal-organic chemical vapor deposition (MOCVD). Independent of growth technique, annealing promotes the formation of In-N bonding, and lateral carrier transport is limited by large scale (\gg mean free path) material inhomogeneities. Comparing solar cell quantum efficiencies for devices grown by MBE and MOCVD, we find significant electron diffusion in the MBE material (reversed from the hole diffusion occurring in MOCVD material), and minority carrier diffusion in InGaAsN cannot be explained by a "universal", nitrogen-related defect.

Introduction

The quaternary alloy, InGaAsN, is a novel material system with many important potential device applications. Opposite to the trend based on the respective bandgaps of GaAs (1.4 eV) and GaN (3.5 eV), addition of a small amount of nitrogen to GaAs radically *lowers* the bandgap.¹⁻³ Addition of indium to GaAsN compensates the strain induced by nitrogen, and with only 3% nitrogen incorporation, one obtains an $\text{In}_x\text{Ga}_{1-x}\text{As}_{1-y}\text{N}_y$ alloy ($x \approx 0.07$, $y \approx 0.03$) with a 1.0 eV bandgap, lattice-matched to GaAs. InGaAsN laser active regions offer the promise of longer wavelength, ≥ 1.3 μm optical transceivers grown on GaAs substrates,^{3,4} or record power efficiencies ($\approx 38\%$) would be obtained with an 1.0 eV, InGaAsN cell added in series to proven InGaP-GaAs tandem solar cells.^{5,6} However, for InGaAsN alloys grown by metal-organic chemical vapor deposition (MOCVD) or molecular beam epitaxy (MBE), photoluminescence intensity and carrier lifetime degrade with increasing nitrogen concentration, and annealing is often required to obtain useful material.^{6,7} Observation of complex annealing behavior in both MBE and MOCVD materials suggests the cause is nitrogen-related defects, not atomic impurities. In this study, we examined the defect and transport properties of MBE and MOCVD-grown InGaAsN. This comparison reveals properties which appear intrinsic to InGaAsN and other characteristics which are unique to a particular growth process. Although the minority carrier properties of MBE and MOCVD-grown InGaAsN differed, comparable solar cell performance was obtained with either growth process.

InGaAsN Growth

$\text{In}_{0.07}\text{Ga}_{0.93}\text{As}_{0.98}\text{N}_{0.02}$ (1.1 eV bandgap) was grown by MBE at a temperature of approximately 430°C. Nitrogen was supplied by a radio-frequency plasma source, while the

remainder of the constituent elements were evaporated from conventional solid sources. Ex-situ, post-growth annealing of this material at 900°C for 10 sec improved the photoluminescence efficiency and subsequent device performance. The MBE material was unintentionally doped, p-type ($\text{mid-}10^{16}/\text{cm}^3$). N-type material was obtained with Si doping.

MOCVD samples were grown using trimethylindium, trimethylgallium, 100% arsine, and dimethylhydrazine sources. N-type material was achieved using tetraethyltin doping. MOCVD samples were annealed at 650°C for 30 minutes. For both MBE and MOCVD-grown InGaAsN, photoluminescence intensity increased $\approx 10\times$ upon annealing undoped material. Overall, photoluminescence of the MBE material displayed characteristics similar to those we have observed for MOCVD samples.⁶ However, the bandgap of the MBE material, observed through photoluminescence or absorption, increased approximately 20 meV due to incremental nitrogen loss during annealing.

Nitrogen Local-Vibrational -Mode Spectroscopy

Looking for a mechanism to explain annealing behavior, we examined nitrogen-related local-vibration-modes (LVMs). Fourier transform infrared transmission spectra are shown for an annealed and as-grown, undoped InGaAsN (1.1 eV) sample grown by MBE (Figure 1). Prior to annealing, a single LVM line is observed at 468 cm^{-1} which corresponds to the Ga-N mode at 470 cm^{-1} reported for GaAs:N.⁸ No evidence for In-N bonds was

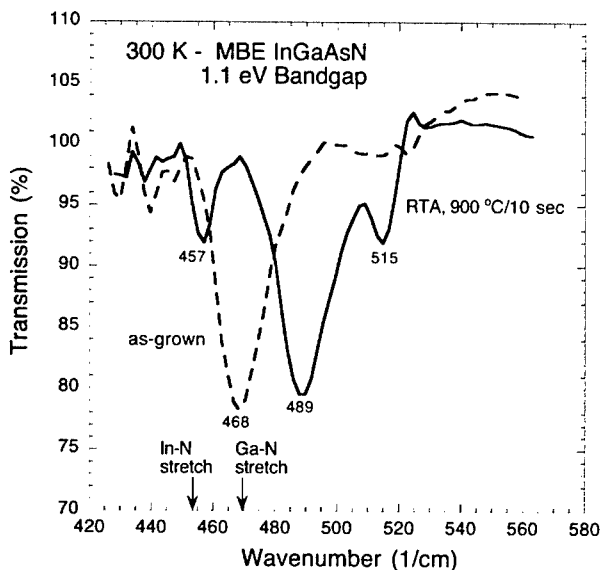


Figure 1. Infrared transmission spectra for an MBE-grown, $0.6\ \mu\text{m}$ thick $\text{In}_{0.07}\text{Ga}_{0.93}\text{As}_{0.98}\text{N}_{0.02}$ sample as-grown (dashed) and ex-situ annealed (solid) at 900°C for 10 sec.

observed prior to annealing. Annealing produced In-N bonds, and three LVMs were observed at 457, 489, and 515 cm^{-1} . With the larger mass of the indium atom, the line at 457 cm^{-1} corresponds to an In-N stretch, and the Ga-N stretch is shifted to 489 cm^{-1} in a Ga_3InN cluster.⁹ Origin of the 515 cm^{-1} line is highly speculative. Similar behavior was reported by Sarah Kurtz et al. in MOCVD-grown (@ 550°C) InGaAsN samples with lower nitrogen content (0.2 %).⁹ They still observed a Ga-N, 470 cm^{-1} , peak after annealing at 700°C for 30 minutes, whereas in our MBE samples that peak disappeared after annealing which indicates that almost 100% of the nitrogen atoms formed In-N bonds. In-N pairing minimizes strain energy in the GaAs-like lattice. Our infrared studies of MOCVD-grown InGaAsN (2% N, 600°C growth) were inconclusive due to broadened and distorted (“Fano”) LVM lineshapes.

Majority Carrier Transport and Localization

We examined the effect of these annealing-induced structural changes on Hall transport. Of particular interest, strong random alloy fluctuations in the InGaAsN conduction band may result in electron localization.¹⁰ Hall mobility measurements were made on a series of compensated MOCVD-grown samples with nominally the same composition, 1.6-1.9% N. N-type (Sn) doping levels were varied in this series to range from as-grown p-type to n-type, mid- $10^{17}/\text{cm}^3$. At 300 K and high carrier densities, the electron mobility curves in Fig. 2(a) converge to $\approx 300 \text{ cm}^2/\text{V s}$. Hole mobilities (Fig. 2(b)) at 300 K ranged even lower, 60-90 $\text{cm}^2/\text{V s}$. Hall mobility and carrier concentration temperature dependence are shown in Figure 3 for a single, n-type MBE-grown sample with nominally the same composition. As before, the highest mobility for the MBE material was $\approx 300 \text{ cm}^2/\text{V s}$, consistent with the limit imposed by alloy scattering at this nitrogen concentration.¹¹

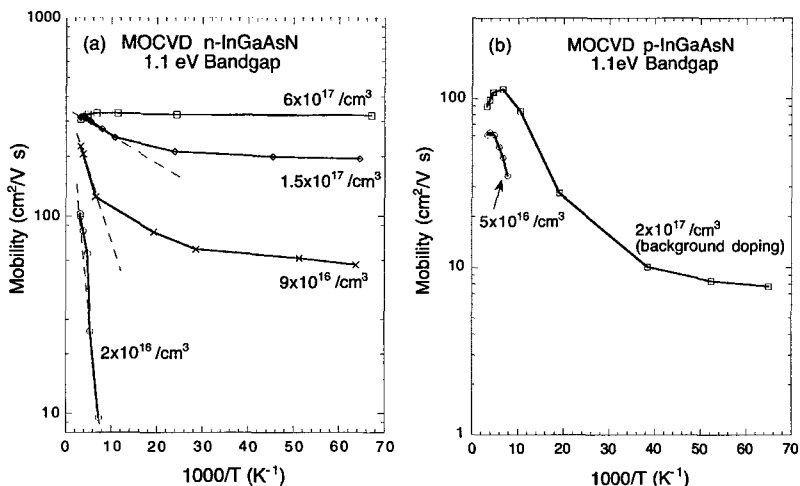


Figure 2. Hall mobility versus temperature for a series of n (a) and p-type (b), MOCVD-InGaAsN samples doped at different levels.

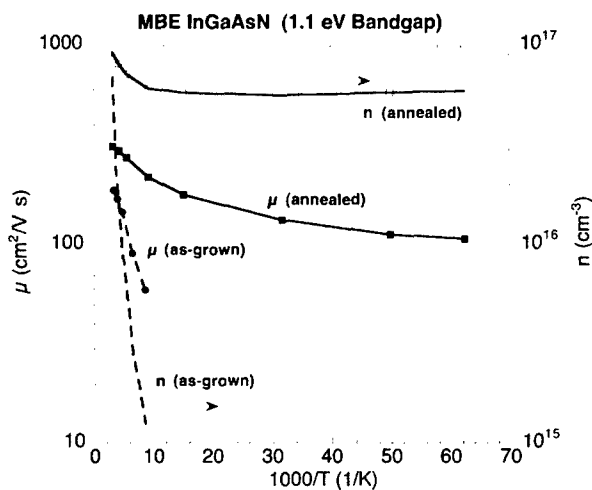


Figure 3. Temperature dependence of Hall mobilities (solid symbol) and carrier concentrations (open symbol) for an MBE-grown, n-type In_{0.07}Ga_{0.93}As_{0.98}N_{0.02} sample as-grown (dashed line) and ex-situ annealed (solid line) at 900°C for 10 sec.

Hall data for the n-type, annealed MBE-grown InGaAsN (Fig. 3) were very close to those for annealed MOCVD material (Fig 2(a)). Electron mobilities (Fig. 2(a)) were thermally activated near 300 K and became weakly temperature dependent at low temperatures. These activation energies increase with decreasing electron concentration (Fig. 2(a)). Based on limited data, we find that hole mobilities (Fig. 2(b)) were qualitatively similar to those observed for the electrons. For both electrons and holes, the carrier concentration was only weakly temperature dependent. Overall, the Hall data for annealed InGaAsN were inconsistent with an electron mobility-edge because: 1) Our Hall mobilities, not carrier concentrations, were thermally activated; 2) Holes displayed similar behavior to electrons; and 3) Low temperature mobility values were large for variable-range hopping.¹² Instead, we believe that InGaAsN carrier transport is modulated by large scale (i.e. \gg mean free path) inhomogeneities, forming potential barriers. Consistent with our data, the Hall mobility is thermally activated in such inhomogeneous materials,¹³ and Hall data for polycrystalline Si are similar to our InGaAsN results.¹⁴ Our results indicate that increased doping (i.e. increasing the Fermi energy) lowers the InGaAsN electron barriers, suggesting inhomogeneities in N concentration (< 1%) produce the barriers. Contrary to reports of a random N distribution occurring in strained, GaAsN (2% N) quantum wells,¹⁵ scanning tunneling microscope images of our MOCVD-InGaAsN revealed N clustering and lateral non-uniformities.¹⁶

In the unannealed, as-grown MBE Hall sample (Fig. 3), we observed strong thermal activation of both mobility and carrier concentration. An activated carrier concentration suggests a trap-modulated mobility with a mobility edge. We associate the localization in as-grown MBE InGaAsN with structural disorder resulting from the lower temperature MBE

growth. Perhaps defects inferred from LVM spectra or excess nitrogen¹⁷ produce localization observed in InGaAsN grown at lower temperature.

Minority Carrier Diffusion and Solar Cells

Minority carrier devices are very sensitive to localization and trapping. To examine the effect of nitrogen-related defects on electron and hole diffusion lengths, we compared structurally similar solar cells, grown by MOCVD or MBE. Our non-optimized, test-cell consisted of a thick (1 μm) InGaAsN base and a thin (0.1-0.3 μm), heavily doped (mid- 10^{17} / cm^3) InGaAsN emitter. Minority carrier diffusion lengths were determined from internal quantum efficiency (IQE) measurements performed on n-on-p and p-on-n solar cells. From the capacitance-voltage, InGaN optical absorption, and IQE spectral data, minority carrier diffusion lengths were determined from device simulations using the program, PC-1D.¹⁸

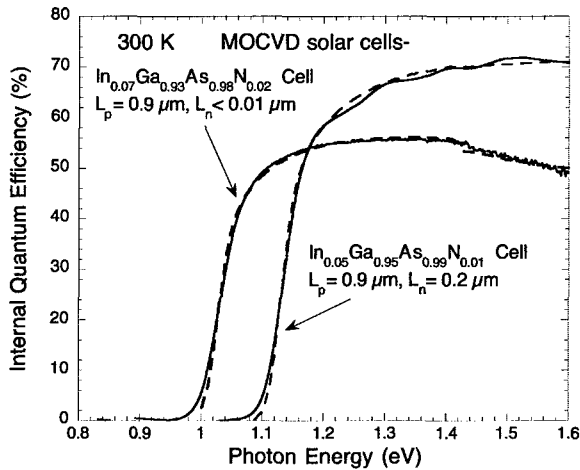


Figure 4. Spectral response of two MOCVD-InGaAsN cells with different alloy compositions (1% and 2% N). Cell simulations (dashed lines) and respective electron (L_n) and hole (L_p) minority carrier diffusion lengths are indicated in the figure.

IQE experimental results and device simulations for MOCVD-grown p-on-n, InGaAsN solar cells with 1.0 eV and 1.1 eV bandgap InGaAsN (2.1% and 1.1% N, respectively) are shown in Figure 4. In the emitter of the 1.0 eV InGaAsN cell, electrons were localized, with a diffusion length $\approx 10^{-2}$ μm , and in the 1.1 eV InGaAsN emitter, electron diffusion had increased to 0.2 μm . In both cells, a hole diffusion length of ≈ 1 μm was obtained for the base layer. Open circuit voltages, at air-mass 0, for the 1.0 eV and 1.1 eV cells were 0.41 and 0.50 V, respectively. IQEs for the companion, n-on-p cells were low (<30%). Clearly, poor electron diffusion limited MOCVD-InGaAsN device performance.

IQE data and simulations for MBE-grown, thick p-base (n-on-p) and thick n-base (p-on-n) are shown in Figure 5. Clearly, the thick p-base devices have higher IQEs indicating

that the minority carrier, electron diffusion length was greater than that of the holes in the MBE-InGaAsN. Self-consistent fits of the cell IQEs were obtained with electron and hole diffusion lengths of 0.5 and 0.03 μm , respectively, in ex-situ annealed MBE material. The air-mass-0, open circuit voltage of the annealed, thick p-base MBE cell in Fig. 5 was 0.43 V. Overall, the IQEs and open circuit voltages of thick p-base MBE and thick n-base MOCVD solar cells were roughly comparable.

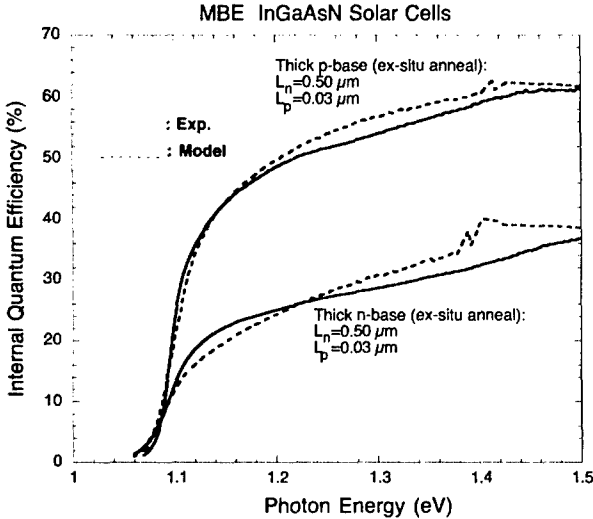


Figure 5. Spectral response of two MBE-grown InGaAsN solar cells, thick p-base (n-on-p, ex-situ annealed) and thick n-base (p-on-n, ex-situ annealed) devices. Cell simulations (dashed lines) and respective electron (L_n) and hole (L_p) minority carrier diffusion lengths are indicated for each cell.

Surprisingly, the diffusion lengths for annealed MBE material were reversed from those we reported for MOCVD-grown InGaAsN (0.01 micron for electrons and 0.9 micron for holes). Although we have presented evidence of point- defects and inhomogeneities common to MBE and MOCVD materials, this variation of minority carrier properties indicates that there are yet other traps associated with each specific growth process.

Summary

Our brief study of the properties of MBE-grown InGaAsN (≈ 1.1 eV bandgap) revealed many similarities to MOCVD material. Overall, the radiative efficiencies, Hall mobilities, device performance, and annealing behavior for MBE and MOCVD-grown InGaAsN were roughly comparable. We found evidence that annealing promotes the formation of In-N bonding like that reported for MOCVD material with lower nitrogen content. Annealed n-type, MBE-grown InGaAsN displayed a Hall mobility temperature dependence like that observed for MOCVD-grown material. We attribute the Hall mobility

temperature dependence to the presence large-scale inhomogeneities, or barriers, limiting transport. The maximum electron mobility was consistent with the limit imposed by alloy scattering, but there was no evidence of alloy-fluctuation-induced-localization. However, some transport properties were unique to a particular growth process. MBE samples grown at lower temperature displayed a strongly thermally activated mobility and carrier concentration only prior to annealing, suggesting trap-modulated transport. In annealed MBE-grown solar cells electron diffusion was dominant (electron and hole diffusion lengths of 0.5 μm and 0.03 μm , respectively), whereas in MOCVD devices the minority carrier diffusion lengths were reversed with holes dominating. In summary, a comparison of MBE and MOCVD material revealed common, intrinsic point-defects and inhomogeneities in InGaAsN, but minority carrier properties of InGaAsN remain unexplained by "universal" defect models.

Acknowledgements

The authors thank J. A. Bur and M. Bridges for technical support. Sandia is a multiprogram laboratory operated by Sandia Corporation, a Lockheed Martin Company, for the U.S. Dept. of Energy under contract DE-AC04-94AL85000.

References

1. M. Weyers, M. Sato, and H. Ando, *Jpn. J. Appl. Phys.* **31 Pt. 2**, 853 (1992).
2. W. G. Bi and C. W. Tu, *Appl. Phys. Lett.* **70**, 1608 (1997).
3. M. Kondow, T. Kitatani, S. Nakatsuka, M. C. Larson, K. Nakahara, Y. Yazawa, and M. Okai, *IEEE J. of Selected Topics in Quant. Elect.* **3**, 719 (1997), and references therein.
4. K. D. Choquette, J. F. Klem, A. J. Fischer, O. Blum, A. A. Allerman, I. J. Fritz, S. R. Kurtz, W. G. Breiland, R. M. Sieg, K. M. Geib, J. W. Scott, and R. L. Naone, *Electron. Lett.* **36**, 1388 (2000).
5. Sarah R. Kurtz, D. Myers, and J. M. Olsen, *Proc. 26th IEEE Photovoltaics Spec. Conf.* (IEEE, New York, 1997), p. 875.
6. Steven R. Kurtz, A. A. Allerman, E. D. Jones, J. M. Gee, J. J. Banas, and B. E. Hammons, *Appl. Phys. Lett.* **74**, 729 (1999).
7. E. V. K. Rao, A. Ougazzaden, Y. Le Bellego, and M. Juhel, *Appl. Phys. Lett.* **72**, 1409 (1998).
8. V. Riede, H. Neumann, H. Sobotta, R. Schwabe, W. Siefert, and S. Schwetlick, *Phys. Stat. Sol.(a)* **93**, K151 (1986).
9. Sarah Kurtz, J. Webb, L. Gedvilas, D. Friedman, J. Geisz, J. Olsen, R. King, D. Joslin, and N. Karam, *Appl. Phys. Lett.* **78**, 748 (2001).
10. Steven R. Kurtz, A. A. Allerman, C. H. Seager, R. M. Sieg, and E. D. Jones, *Appl. Phys. Lett.* **77**, 400 (2000).
11. C. Skierbiszewski, P. Perlin, P. Wisniewski, T. Suski, W. Walukiewicz, W. Shan, J. W. Ager, E. E. Haller, J. F. Geisz, D. J. Friedman, J. M. Olsen, and S. R. Kurtz, *Phys. Stat. Sol.(b)* **216**, 135 (1999).
12. N. F. Mott and E. A. Davis, *Electronic Processes in Non-Crystalline Materials*, 2nd Ed., Clarendon Press, Oxford, 1979
13. V. G. Karpov, A. Ya. Shik, and B. I. Shklovski, *Sov. Phys. Semi.* **16**, 901 (1982).

14. H. Paul Maruska, Amal K. Ghosh, Albert Rose, and Tom Feng, *Appl. Phys. Lett.* **36**, 381 (1980).
15. H. A. McKay, R. M. Feenstra, T. Schmidtling, and U. W. Pohl, *Appl. Phys. Lett.* **78**, 82 (2001).
16. H. Lyeo, C. K. Shih, A. A. Allerman, S. R. Kurtz, and E. D. Jones, to be published
17. Sylvia G. Spruytte, Christopher W. Coldren, James S. Harris, William Wampler, Peter Krispin, Klaus Ploog, and Michael C. Larson, *J. Appl. Phys.* **89**, 4401 (2001).
18. PC1D Version 5.2, Copyright P. A. Basore and D. A. Clugston, Univ. of New South Wales, Aus. (1998).